Solvent dielectric effects on isomerization dynamics: Investigation of the photoisomerization of 4,4'dimethoxystilbene and tstilbene in nalkyl nitriles

N. Sivakumar, E. A. Hoburg, and D. H. Waldeck

Citation: The Journal of Chemical Physics **90**, 2305 (1989); doi: 10.1063/1.455971
View online: http://dx.doi.org/10.1063/1.455971
View Table of Contents: http://scitation.aip.org/content/aip/journal/jcp/90/4?ver=pdfcov
Published by the AIP Publishing

Articles you may be interested in

Viscosity dependence and solvent effects in the photoisomerization of cis-stilbene: Insight from a molecular dynamics study with an ab initio potential-energy function
J. Chem. Phys. **111**, 8987 (1999); 10.1063/1.480242

Computer simulation of the photoisomerization dynamics of stilbene
AIP Conf. Proc. **364**, 54 (1996); 10.1063/1.50169

Implications for multidimensional effects on isomerization dynamics: Photoisomerization study of 4,4' dimethylstilbene in nalkane solvents
J. Chem. Phys. **91**, 943 (1989); 10.1063/1.457146

Evidence for dynamical solvent dielectric effects: Photoisomerization of stilbenes
AIP Conf. Proc. **172**, 634 (1988); 10.1063/1.37495

Photoisomerization of stilbene in low viscosity solvents: Comparison of isolated and solvated molecules
J. Chem. Phys. **83**, 215 (1985); 10.1063/1.449811

This article is copyrighted as indicated in the article. Reuse of AIP content is subject to the terms at: http://scitation.aip.org/termsconditions. Downloaded to IP: 130.88.90.140 On: Thu, 18 Dec 2014 22:34:06

Solvent dielectric effects on isomerization dynamics: Investigation of the photoisomerization of 4,4′-dimethoxystilbene and *t*-stilbene in *n*-alkyl nitriles

N. Sivakumar, E. A. Hoburg, and D. H. Waldeck
Department of Chemistry, University of Pittsburgh, Pittsburgh, Pennsylvania 15260

(Received 16 September 1988; accepted 9 November 1988)

New data for the photoisomerization dynamics of *t*-stilbene and 4,4′-dimethoxystilbene in polar solvents are reported. These data demonstrate that in *n*-alkyl nitriles, nonassociated polar solvents, it is possible to extract a solvated barrier for the isomerization. This result is contrasted with recent studies in *n*-alkyl alcohols, associated polar solvents, where this separation is not possible and clarifies the origin of the changing barrier height in *n*-alkyl alcohols. Comparison of reduced isomerization rates with models of chemical reaction dynamics in solution are drawn. Good agreement of the data with a coupled oscillator model is found.

INTRODUCTION

The *trans* to *cis* photoisomerization of stilbene[1–6] and its analogs[7,8] provides a model system for the investigation of unimolecular reactions in the condensed phase. These studies have pointed to two primary solvent effects on the isomerization, namely solute/solvent friction and solute/solvent dielectric interactions. The incorporation of these effects into a proper modeling of the reaction dynamics is still developing. For instance, it remains to be ascertained under what conditions stochastic models (such as Kramers) are appropriate, or alternatively under what conditions non-Markovian effects become important to the dynamics.[9–11]

The isomerization of stilbenes involves a large amplitude motion which couples to the solvent through collisions, i.e., friction. Experimental studies of *t*-stilbene in nonpolar solvents have elucidated both the regime where the reaction rate increases with solvent friction[4] and the regime where the reaction rate decreases with solvent friction. This latter regime, the more common in liquid solution, is considered in this study. Furthermore, studies in nonpolar solvents indicate that the intramolecular potential energy barrier and the solvents' frictional influence are separable. In fact, the size of the potential energy barrier for stilbene in alkane solvents agrees closely with the isolated molecule value.[12] Investigations of the isomerization of stilbenes and other compounds in the solvent damping regime (rate decreases as friction increases) have revealed deviations from the predictions of Kramers model when shear viscosity is used as a measure of solute/solvent friction. Although a variety of approaches have been used to better model the friction, the limits of applicability of Kramers model remain unclear.[3(b)]

A second aspect of the solvents' influence occurs through the dielectric properties of the solvent. The isomerization of stilbenes is believed to involve a very polar, twisted intermediate[13] and the excited state potential energy surface of stilbene is strongly influenced by polar solvents. A variety of studies in polar solvents[5–7,14–17] show the dramatic influence of solvation on the activation barrier to isomerization. Photoisomerization studies on *t*-stilbene[5] and 4,4′-dimethoxystilbene (DMS)[7] in *n*-alcohol solvents have revealed that the solvent friction and barrier influences are not separable, as for the case of nonpolar solvents. It was suggested in this earlier work that this loss of separability arose because of the slow dielectric response of the *n*-alkyl alcohol solvents (a result of hydrogen-bonded oligomer structures in these solvents). The early time behavior of the fluorescence decay of DMS in *n*-alkyl alcohols[7] can be highly nonexponential, indicating that isomerization and solvation of the excited state are occurring on similar time scales. This lack of time scale separation and strong solute/solvent coupling results in an inability to model the reaction as occurring on a one-dimensional equilibrated potential energy surface. These results motivated the present studies which investigate the photoisomerization of *t*-stilbene and 4,4′-dimethoxystilbene in the *n*-alkyl nitrile solvents.

Because the nitriles are polar but nonassociating, effects of solvation on the barrier will be present but the dielectric response should be rapid.[18] Excited state lifetime studies have been performed for both *t*-stilbene and DMS in the homologous series of *n*-alkyl nitriles from propionitrile to decanenitrile as a function of temperature at ambient pressure. For both stilbene and DMS it is possible to extract an effective barrier (solvated barrier) from the data. This solvated barrier to isomerization is reduced in magnitude from that observed in alkanes.

The rest of this manuscript is organized as follows. First, specific experimental details are discussed. Second, the data analysis used to successfully separate the activation barrier from solvent friction effects is presented. Subsequent to this separation, comparisons are drawn between the measured frequency factors and a hydrodynamic Kramers model. Fourth, the data is analyzed in terms of "extended" Kramers models. That is, models which have a Kramers form, but with a more detailed treatment of the friction. Lastly, the conclusions and implications of this work are discussed.

EXPERIMENTAL

Measurement of fluorescence decay rates k_F and quantum yields ϕ for 4,4′-dimethoxystilbene and *t*-stilbene allowed the isomerization rates k_{iso} to be determined, via

$$k_{iso} = k_F(1 - \phi).$$

 0021-9606/89/042305-12$02.10 © 1989 American Institute of Physics

This article is copyrighted as indicated in the article. Reuse of AIP content is subject to the terms at: http://scitation.aip.org/termsconditions. Downloaded to IP: 130.88.90.140 On: Thu, 18 Dec 2014 22:34:06

Fluorescence decay profiles were measured using the time correlated single photon counting technique[19] at a variety of temperatures and ambient pressure. Figure 1 shows a sample decay curve for *t*-stilbene in butanenitrile at a temperature of 284 K. The best fit excited state decay time is 64 ps. This decay curve shows not only the excited state decay but background fluorescence from the solvent. A best fit to a sum of exponentials gives a $\chi^2 = 1.6$ and indicates that the background fluorescence from the solvent. A best fit to a sum of exponentials gives a $\chi^2 = 1.6$ and indicates that the background solvent fluorescence is 0.08% of the signal fluorescence. Fitting of the decay curves to a single exponential vs a double exponential only had a minor effect (<2 ps) on the decay time extracted. Because of the limited instrument response function (60 ps FWHM and 110 ps FWTM) and difficulties in fitting, only experimental conditions which result in decay constants of greater than 30 ps are reported. The specifics of the apparatus used for these studies have been described previously.[7]

Relative quantum yields were measured using an SLM 8000 (SLM Instruments Inc.) fluorimeter in the 90° configuration. The reference standard for these measurements was quinine sulfate in 0.1 N H_2SO_4 ($\phi = 0.54$),[20] the quantum yield of fluorescence of 4,4'-dimethoxystilbene was determined in acetonitrile ($\phi = 0.26$) and in hexanenitrile ($\phi = 0.32$) at 298 K. The radiative rates k_r were determined to be 0.73 ns^{-1} in acetonitrile and 0.62 ns^{-1} in hexanenitrile. The average radiative rate (0.36 ns^{-1} at unit index of refraction) was used in the different nitrile solvents after correcting for the solvent index of refraction [i.e., k_r (ns^{-1}) $= 0.36\ n^2$, where n is the solvents' index of refraction]. The radiative rate for *t*-stilbene, taken to be 6.2×10^8 s^{-1} in *n*-hexane,[2-4] was corrected for index of refraction changes as well.

The *n*-alkyl nitrile solvents required extensive purification before use (solvents were purchased from the Aldrich Chemical Company and Dixon Fine Chemicals). The purification method of choice was to vacuum distill the solvents at temperatures of less than 370 K.[21] The solvents were distilled up to three times. The criterion for purity was that the observable impurity solvent background fluorescence be less than 0.1% of the signal fluorescence. The purification procedure for 4,4'-dimethoxystilbene has been described previously.[7] Scintillation grade *t*-stilbene was used without additional purification. Measurement of the fluorescence lifetime of *t*-stilbene in pentane provided a decay time ($\tau_F = 65$ ps at $T = 295$ K) in close agreement with other workers.[3]

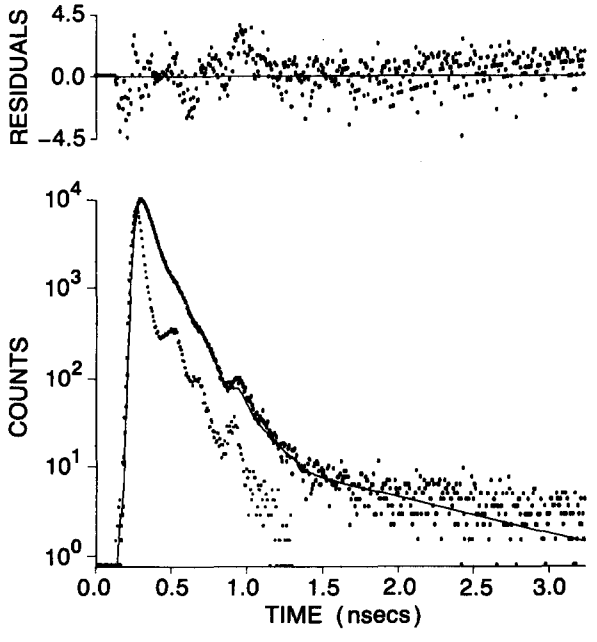

FIG. 1. This figure shows a fluorescence decay curve for *t*-stilbene in *n*-butanenitrile at 284 K. The best fit parameters are given in the text.

The viscosities of *n*-alkyl nitriles were obtained from the literature for propionitrile through hexanenitrile[22] for temperatures greater than 273 K. Viscosities for these solvents were measured from 253 to 273 K and the viscosities of *n*-heptanenitrile through *n*-decanenitrile were measured from 253 to 353 K at ambient pressure using a Uhbolode viscometer. The measured viscosity values for these solvents are reported in the Appendix. The densities for these solvents were obtained from the literature.[23] If densities were not available below 0 °C, they were extrapolated by no more than 25 °C from a fit to the literature data.

The methods used in fitting data have been described elsewhere.[7,24]

EXTRACTION OF SOLVATED BARRIER

The method used to separate the activation barrier from the solvent frictional effects is based on a general expression for the isomerization rate constant, which has an Arrhenius-type form. This expression can be written as

$$k_{iso} = F(\zeta)\exp(-E/RT), \tag{1}$$

where E is the activation energy, R is the gas constant, T is the temperature, and $F(\zeta)$ is a function of the solute/solvent friction ζ and properties of the solute potential energy surface. Because of solute/solvent dielectric interactions, this potential energy surface is not strictly intramolecular. By measuring the isomerization rate constant in an homologous series of solvents, it is possible to perform an Arrhenius plot where the preexponential factor $F(\zeta)$ is held constant. That is, one assumes that the solute potential energy surface pa-

TABLE I. Isoviscosity plot parameters for *n*-alkyl nitriles.

	t-stilbene		4,4'-dimethoxystilbene	
Viscosity (cP)	E (kcal/mol)	Solvents	E (kcal/mol)	Solvents
0.50	...	...	4.18 ± 0.12	C_3–C_7
0.70	2.59 ± 0.13	C_3–C_7	4.04 ± 0.08	C_4–C_{10}
0.90	2.36 ± 0.12	C_4–C_{10}	3.97 ± 0.06	C_5–C_{10}
1.10	2.47 ± 0.08	C_4–C_{10}	3.98 ± 0.10	C_6–C_{10}
1.30	2.53 ± 0.10	C_5–C_{10}	4.26 ± 0.12	C_7–C_{10}
1.50	2.61 ± 0.08	C_5–C_{10}	4.34 ± 0.12	C_8–C_{10}
2.00	2.67 ± 0.06	C_6–C_{10}	...	...
2.50	2.83 ± 0.06	C_7–C_{10}	...	...
3.00	2.54 ± 0.13	C_7–C_{10}	...	...
4.00	2.66 ± 0.19	C_8–C_{10}	...	...
5.00	2.69 ± 0.08	C_8–C_{10}	...	...

This article is copyrighted as indicated in the article. Reuse of AIP content is subject to the terms at: http://scitation.aip.org/termsconditions. Downloaded to IP: 130.88.90.140 On: Thu, 18 Dec 2014 22:34:06

rameters remain constant for all members of the homologous series. If the temperature dependence of the isomerization rate is studied in each member of the homologous series, then it is possible to take a constant friction [and hence constant $F(\zeta)$] slice through the data set. These "isofriction" plots typically involve the assumption that $\zeta \propto \eta_0$, where η_0 is the solvents' zero frequency shear viscosity. The insensitivity of the activation energy, which is obtained from this type of analysis, to the precise modeling of ζ has been discussed and demonstrated for the *n*-alkanes.[7] Previous studies in *n*-alkane solvents found an activation barrier of 3.5 kcal/mol[2,3] for *t*-stilbene and an activation barrier of 5.7 kcal/mol[7] for 4,4'-dimethoxystilbene.

Following this procedure, isoviscosity plots were performed for both 4,4'-dimethoxystilbene and *t*-stilbene in the *n*-alkyl nitriles. Figure 2(a) shows representative plots for *t*-stilbene and Table I provides a listing of the barrier heights (the average barrier height is 2.6 kcal/mol). Figure 2(b) shows representative plots for 4,4'-dimethoxystilbene in *n*-alkyl nitriles and Table I provides a listing of the isoviscosity plots performed. An average value of 4.2 kcal/mol is found for 4,4'-dimethoxystilbene from this analysis. The error in these average barriers is estimated to be $\pm$ 0.2 kcal/mol. For both solute molecules the isomerization barrier is reduced from that seen in *n*-alkane solvents by about 25%. This reduction is in keeping with the presence of a polar transition state which is stabilized in a higher polarity solvent.

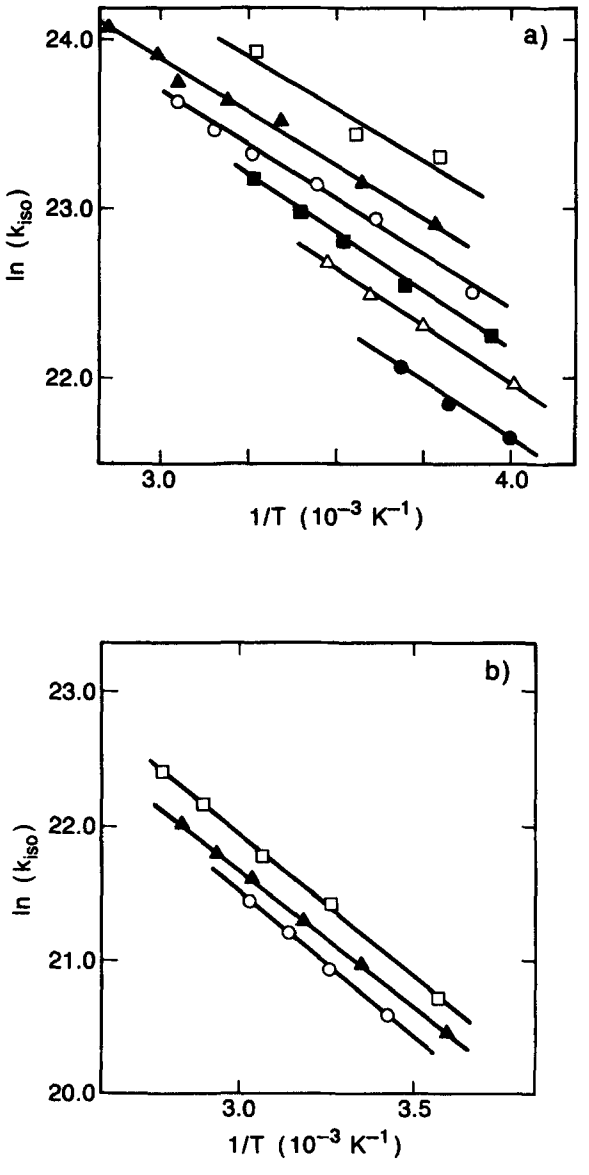

FIG. 2. Isoviscosity plots for (a) *t*-stilbene in the *n*-alkyl nitriles and (b) 4,4'-dimethoxystilbene in the *n*-alkyl nitriles (●: 5.0 cP; △: 3.0 cP; ■: 2.0 cP; ○: 1.3 cP; ▲: 0.9 cP; □: 0.5 cP).

The degree of solvation in different members of the *n*-alkyl nitriles series might be expected to vary and hence the barrier height change through the series.[15] If this effect were strongly manifest in the data, the slopes of the isoviscosity plots would be expected to increase as one progresses from low viscosity to high viscosity. This result would occur because the low viscosity plots involve the more polar members of the series (hence lower barriers) and the high viscosity plots involve the less polar members of the series (hence higher barriers). Hicks *et al.*[15] have proposed a method of correcting for the differing degrees of solvation by different polarity solvents through the use of an empirical polarity scale $E_T(30)$.[25] Performance of that analysis on the isomerization data of 4,4'-dimethoxystilbene and *t*-stilbene does not improve the quality of the isoviscosity plots significantly, although it does shift the average value of the barrier more toward that observed in *n*-alkane solvents, as expected. It is likely that this effect is weak because of the relatively small polarity change through the nitrile series, from an $E_T(30) = 46.0$ for acetonitrile to an $E_T(30) = 40$ for nonanenitrile. In fact, the range of polarity through the nitrile series is not much different than that of the *n*-alkanes. The work of Brady and Carr[26] shows that on the π^* polarity scale the alkanes range from $\pi^* = -0.08$ for pentane to $\pi^* = 0.08$ for hexadecane, as compared to a range of $\pi^* = 0.75$ for acetonitrile to $\pi^* = 0.62$ for decanenitrile. Although the nitriles are on the average much more polar than the alkanes the variation of polarity through the homologous series is similar.

The insensitivity to polarity changes through the homologous series of *n*-alkyl nitriles can be further examined through the steady state Stokes shift of 4,4'-dimethoxystilbene in the *n*-alkyl nitriles. Table II shows the steady state

TABLE II. Steady state spectral data for 4,4'-dimethoxystilbene in *n*-alkyl nitrile solvents.

Solvent	λ_{abs}[a] (nm)	λ_{fl}[a] (nm)	SS[b] (cm^{-1})
Propionitrile	325.9	375.1	226
Butanenitrile	326.1	375.6	242
Pentanenitrile	326.9	375.2	139
Hexanenitrile	327.1	376.3	198
Heptanenitrile	327.0	376.7	236
Octanenitrile	326.5	376.5	268
Nonanenitrile	327.5	376.6	182
Decanenitrile	···	376.0	···

[a] The wavelength is the maximum of the absorption or fluorescence profile.
[b] The Stokes shift is defined relative to the *n*-alkanes (see the text for details). The error in this number is estimated to be $\pm$ 50 cm^{-1}.

This article is copyrighted as indicated in the article. Reuse of AIP content is subject to the terms at: http://scitation.aip.org/termsconditions. Downloaded to IP: 130.88.90.140 On: Thu, 18 Dec 2014 22:34:06

spectral data for this solute in the alkyl nitriles at 25 °C and ambient pressure. Because of the difficulty in assigning the 0–0 transition, the Stokes shifts are determined by computing the energy difference between the absorption and fluorescence peaks. The Stokes shift for DMS is reported with respect to the average value of this shift in the *n*-alkane series, namely 3799 cm^{-1}.[7] To the extent that there is no orientational ordering of the alkane solvent about the DMS, the value of the Stokes shift reported here provides a measure of the orientational polarization about the solute in the *n*-alkyl nitriles. As observed with both the alcohols and alkanes,[7] the steady state spectral data in the nitriles indicates that the solvation is dominated by the optical part of the solvent response. That is, both the absorption and fluorescence peak positions show a red shift as the index of refraction of the solvent increases. Such behavior indicates that the initially prepared excited state has a small dipole moment and/or small change in geometry, and is well approximated as the *trans* species. It is expected that the *t*-stilbene Stokes shift would behave in a similar manner.

The isoviscosity plots presented here suggest that the attempt to separate the energy barrier and solvent frictional effects on the isomerization rate is successful. Although the barrier height obtained is smaller than the corresponding barrier in alkanes (which is very close to that of the isolated molecule), this difference can be explained by an increased solvation of the transition state by the more polar nitrile solvents. Whether or not the activation barrier obtained corresponds to an equilibrium solvation barrier remains unclear. Although the barrier could correspond to the equilibrium value, it may well be that it is an effective barrier and the system is actually nonequilibrium. Because the degree of solvation and the time scale of the dielectric response[18,27] is similar throughout the homologous series, the barrier height appears to be constant in the isoviscosity plots. This extraction of a barrier is in direct contrast to observations in alcohol solvents. In the *n*-alkyl alcohols the isoviscosity plots' slopes (activation energies) change for differing viscosities.[5,7] In fact, as the viscosity increases the slope becomes shallower. Although it might first appear that the barrier is viscosity dependent as reported for other species,[16] the nitrile studies demonstrate that this is not so. The isoviscosity plots for the nitriles have been performed over the same viscosity range as the *n*-alcohol studies, but the activation barriers obtained are constant. These results identify the changing barrier in the *n*-alkyl alcohol studies to be associated with the large change in polarity through the alcohol series and/or the slow dielectric relaxation of the alcohols.

DISCUSSION

Equation (1) gives a general form of the rate constant in terms of a preexponential factor and an activation term. Having obtained the activation barrier through the use of the isoviscosity plots, it is now possible to extract the preexponential factor $F(\zeta)$ from the data and compare the experimental values of $F(\zeta)$ with the predictions of various models.

Kramers' model

A prevalent model for the reduced isomerization rate constant is that of Kramers.[9] In this model the reactive flux (flux of probability) is found for a Brownian particle diffusing over a potential barrier in one dimension. A description of the assumptions and limitations of this model have been given previously.[7,9–11] Solving the Fokker–Planck equation for this motion results in

$$F(\zeta) = \frac{\omega_0 \zeta}{4\pi\omega_b I_r}\left\{\left[1+\left(\frac{2\omega_b I_r}{\zeta}\right)^2\right]^{1/2}-1\right\}. \qquad (2)$$

Although it is typical to associate the activation barrier with an intramolecular barrier, for the case of the alkyl nitriles it should be considered an effective, or solvated barrier. In this expression, ω_0 is the reactant well frequency, ω_b is the barrier frequency, I_r is the effective mass of the particle (for the isomerization, a reduced moment of inertia), and ζ is the solute/solvent friction. In order to compare the measured rate constants with Eq. (2) it is necessary to model the friction ζ. In particular, by assuming that ζ is proportional to the solvent shear viscosity η_0, Eq. (2) can be converted to a hydrodynamic form

$$F(\zeta) = \frac{A}{B/\eta_0}\{[1+(B/\eta_0)^2]^{1/2}-1\}. \qquad (3)$$

This assumption of using a macroscopic parameter η_0 to describe the microscopic solute–solvent friction has serious limitations which have been discussed by a number of workers.[2,3,7,28,29]

The hydrodynamic Kramers form has been fit to the data for both *t*-stilbene (dashed line in Fig. 3) and for 4,4′-dimethoxystilbene (dashed line in Fig. 4). The behavior illustrated in these fits has been observed in a variety of other studies, as well. The Kramers form does not possess enough curvature to fit the data. If a best fit is performed to the low viscosity data the line underestimates the rate at high viscosity and, conversely, if the model is fit to the high viscosity data it underestimates the rate at low viscosities. This failure could result from a variety of sources, among which are the hydrodynamic form of the friction, the use of a zero frequency measure of the friction, and the use of a one-dimensional model. These limitations are discussed further below.

Before proceeding, it is useful to discuss the fit of the data to a phenomenological functional form, namely

$$F(\zeta) = B/\eta_0^a. \qquad (4)$$

Fits of the data to this power law form are found to be good for a variety of systems. The parameter a gauges the strength of the solvent damping and B indicates the frequency, or time scale, of the isomerization motion. Although these parameters are not interpretable directly because of the lack of a physical model, they allow comparison between systems in order to identify general trends. The solid line in Fig. 3 shows the best fit of Eq. (4) to the *t*-stilbene in nitriles data and the best fit parameters are $B = 1.1\times10^{12}$ s^{-1} at 1 cP and $a = 0.51$. Figure 4 shows a best fit of Eq. (4) to the dimethoxystilbene in nitriles data with best fit parameters of $B = 1.4\times10^{12}$ s^{-1} at 1 cP and $a = 0.44$. The major error in these fitting parameters is systematic error caused by the choice of an activation barrier. For changes in the activation energy of $\pm$ 0.5 kcal/mol the a parameters change by less than 0.015. These parameters are in keeping with the conclusions of previous studies on *t*-stilbene and 4,4′-dimethoxys-

This article is copyrighted as indicated in the article. Reuse of AIP content is subject to the terms at: http://scitation.aip.org/termsconditions. Downloaded to IP: 130.88.90.140 On: Thu, 18 Dec 2014 22:34:06

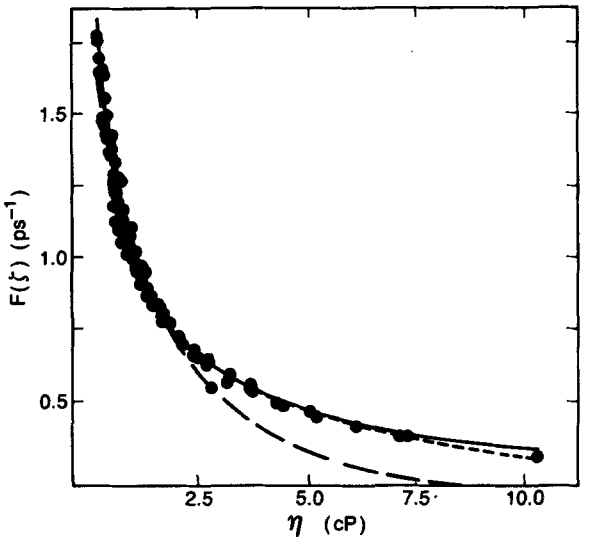

FIG. 3. Plot of the reduced isomerization rate data of *t*-stilbene in *n*-alkyl nitriles vs the zero frequency shear viscosity of the solvent. The long dashed curve is the best fit to Kramers model; the short dashed curve is the best fit to Eq. (10); the solid line is the best fit to a power law form [Eq. (4)].

tilbene in *n*-alkanes[2,3,7] and from other solute systems,[29–31] as well. Namely, as the barrier height increases (DMS has a 4.2 kcal/mol barrier and *t*-stilbene a 2.6 kcal/mol barrier), the frequency of the motion increases (gauged by the magnitude of B) and the viscosity dependence becomes weaker (a decreases). The conclusions drawn from this correlation are that the friction dependence of the isomerization is frequency dependent. That is, the friction which should be used in describing the isomerization is the friction evaluated at the characteristic frequency of the reaction.[10,32,33] Because the zero frequency shear viscosity of the solvent incorporates both high and low frequency solvent motions it is the incorrect friction to use. On the reaction time scale the low frequency motions of the solvent contribute very little to the solute/solvent friction, hence as the frequency of the motion increases the zero-frequency shear viscosity becomes a worse measure of the friction. In keeping with previous studies, it is observed here that as the barrier height increases the frequency of the motion becomes higher and the viscosity dependence of the reduced isomerization rate is weaker.

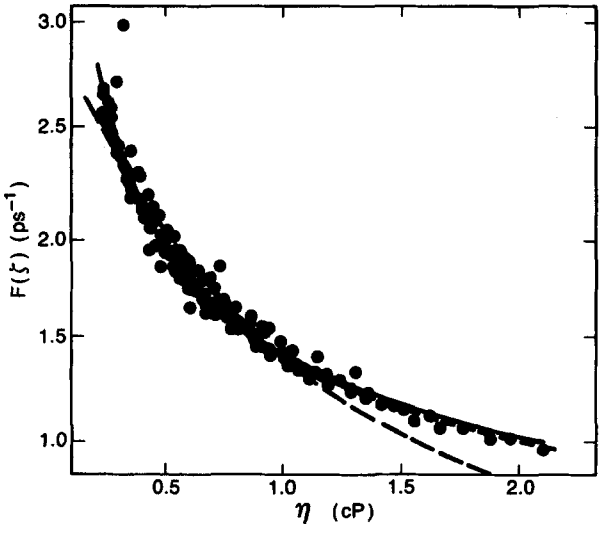

FIG. 4. Plot of the reduced isomerization rate data of 4,4'-dimethoxystilbene in *n*-alkyl nitriles vs the zero frequency shear viscosity of the solvent. The long dashed curve is the best fit to Kramers model; the short dashed curve is the best fit to Eq. (10); the solid line is the best fit to a power law form [Eq. (4)].

For the particular case of 4,4'-dimethoxystilbene and *t*-stilbene in *n*-alkyl nitriles, a behavior similar to the *n*-alkane case is observed. Even though the viscosity dependence in the *n*-alkyl nitriles is correspondingly larger than in the *n*-alkanes, the ordering of the viscosity dependence within a solvent type is the same. The trend is that *t*-stilbene has a stronger viscosity dependence than 4,4'-dimethoxystilbene. This observation is in direct contrast to the predictions of free volume theories of the friction, which give rise to a functional form of the type in Eq. (4).[7,34] Qualitatively it would be expected that if the displaced volume of the motion is larger, then the viscosity dependence should be stronger. This intuition is supported by recent studies of the dependence of the rotational diffusion of solute probes on the solute-to-solvent size ratio.[35,36] Using van der Waals radii, it appears that 4,4'-dimethoxystilbene should displace twice as much volume upon isomerization than does *t*-stilbene, yet, it has a weaker viscosity dependence. Perhaps in this situation, the effects of a frequency dependence on the friction override the spatial aspect of the friction.

An aspect of the Kramers model which has been tested in a variety of ways is the modeling of the solute/solvent friction. One straightforward approach is to use a more microscopic measure of the solute/solvent friction rather than the solvent shear viscosity. In particular, workers have used the overall rotational diffusion time of the solute τ_{or} as a measure of the friction for the isomerization in the case of *t*-stilbene in alkanes,[2,3] the dye molecule DODCI in alcohols,[29] and binaphthyl in alkanes and alcohols.[28] For the case of *t*-stilbene in *n*-alkane solvents this approach leads to a small improvement in the best fit to Kramers model but does not totally correct for the limitations of the Kramers treatment. For the case of DODCI in *n*-alkyl alcohols there is no improvement in the fits. In the case of binaphthyl the use of τ_{or} seems to model the friction appropriately, and good agreement with Kramers' model is observed. However, in *n*-alcohol solvents, η_0 models the friction just as well as τ_{or}. It is important to note that because binaphthyl has a lower barrier to isomerization (< 1.4 kcal/mol), frequency dependent effects may be less important. A different type of treatment has been attempted for the case of 4,4'-dimethoxystilbene in *n*-alkanes. The light scattering relaxation time of the solvent, a measure of the solvent/solvent friction on a microscopic scale, was used as a measure of the microscopic solute/solvent friction.[7] Little improvement was observed for this treatment, as well. The underlying tenet of these approaches seems valid, however. That is, one should model the spatial and dynamic aspects of the solute/solvent friction appropriately before conclusions can be drawn concerning the adequacy of a Kramers type of treatment.

This article is copyrighted as indicated in the article. Reuse of AIP content is subject to the terms at: http://scitation.aip.org/termsconditions. Downloaded to IP: 130.88.90.140 On: Thu, 18 Dec 2014 22:34:06

For the case of *n*-alkyl nitriles the Debye relaxation time τ_d of the solvent can be used to gauge the solvent/solvent friction on a more microscopic time and distance scale than does the zero frequency shear viscosity. Because the amount of dielectric relaxation data on nitriles is limited, it is necessary to estimate these times from a Stokes–Einstein Debye[37] model of the relaxation. The measured dielectric relaxation data in acetonitrile[27] was fit to

$$\tau_d(\text{ps}) = C\eta_0/T + \tau_0,$$

where C and τ_0 are adjustable parameters. The constant C depends on the molecular shape, volume, and hydrodynamic boundary conditions employed. The Debye relaxation time in other *n*-alkyl nitrile solvents is estimated by correcting the constant C for the increasing solvent volume through the homologous series. The use of the relaxation times from this modeling differs from the use of shear viscosity by the change in C and the presence of the constant term τ_0. Use of this characteristic relaxation time for the friction in the standard Kramers expression does not improve the agreement with the data.

For a variety of solute species the overall rotational motion is found to scale linearly with η_0/T in a *single* solvent.[35,36] This behavior is observed even in the case of solute particles which are close to or smaller than the solvent, i.e., even when the reorientational motion may not be small step diffusion.[35,36,38] The success of a hydrodynamic model in this restricted regime for overall rotational motion suggests that such a modeling would be appropriate for isomerization in a single solvent. As recently shown by Kim *et al.*[3(b)] for *t*-stilbene in decane the Kramers model with a zero frequency hydrodynamic friction still fails. Figure 5 shows two such fits for *t*-stilbene in decanenitrile and in octanenitrile. The decanenitrile case shows quite dramatically the failure of a Kramers-type model. Although the linearity of the overall rotational relaxation time τ_{or} of *t*-stilbene with shear viscosity in decanenitrile has not been verified, substantial circumstantial evidence suggests it would be linear. The best evidence for the presumed linearity is the work of Kim[3(b)] which found τ_{or} to be linear with viscosity in decane. Since decane and decanenitrile are of like size, the solute/solvent size ratio should be similar for the two cases. This ratio is a primary cause of a nonlinear dependence on viscosity.[35]

These deviations are not present in all solvents, however. If the viscosity range spanned is small enough, then the Kramers model can be made to fit the data. Figure 5 shows an example fit for *t*-stilbene in octanenitrile and similar quality fits can be performed for *t*-stilbene in octane, DMS in octanenitrile, and DMS in octane. Through the use of a structural model for the isomerizing particle, parameters of the potential energy surface can be obtained from these fits. The structural parameters used here are similar to those of other workers.[2,3,39] For *t*-stilbene the reduced moment of inertia I_r is taken to be 0.433×10^{-44} kg m^2. The hydrodynamic radius of the isomerizing moiety R is taken to be 3.2 Å and the distance of the center of the moiety from the axis of rotation D is taken to be 2.5 Å. For 4,4′-dimethoxystilbene the parameters are estimated to be 1.01×10^{-44} kg m^2, 3.7 Å, and 3.5 Å, respectively. Table III provides best fit Kramers parameters for the different solute/solvent combinations with these structural parameters and a slip hydrodynamic boundary condition for determination of the friction coefficient.[2,3,40] Although the potential parameters give physically reasonable values in all cases, the trend for the barrier curvature between species is unreasonable. For the case of *t*-stilbene as one goes from *n*-octane to *n*-octanenitrile the barrier height decreases, but the barrier curvature obtained from the Kramers fit increases. This trend is unphysical. Although the friction in the latter solvent (octanenitrile) may be different than octane, in order to reverse the trend of the barrier curvature one must actually decrease the frictional coupling in the octanenitrile compared to the octane, which is unreasonable as well. Because the structural constants (I_r, R, D) of the stilbene should not change in different solvents, it is possible to rescale ω_0 and ω_b using the barrier height changes and fit the data in octane and octanenitrile simultaneously. Fits of this type are extremely poor. Comparisons between solute types in octanenitrile seem unreasonable as well, namely the barrier frequency obtained for DMS is half that of *t*-stilbene despite the higher barrier for DMS in octanenitrile. This latter trend is not necessarily unrealistic since the moment of inertia of DMS is more than twice that of *t*-stilbene and the distance scale is not strictly the same between the solutes. However, the trend in ω_0 values is in the opposite direction. Lastly, the trend in barrier frequencies between solute types is different for the two different solvent systems (octane vs octanenitrile) as well. A caveat to these comparisons is that the octane data spans a small range of viscosity and there could be considerable error in these best fit parameters. In conclusion, although Kramers model can be made to fit the data over a small viscosity range with physically reasonable potential surface parameters, the trends one observes between solute types and between solvent types are unreasonable.

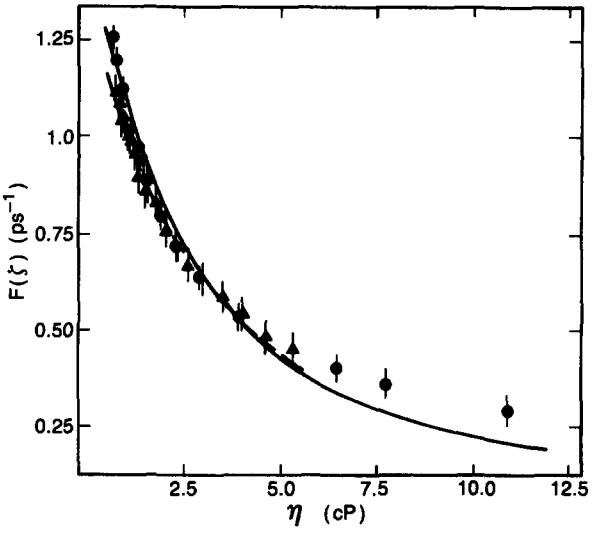

FIG. 5. Best fit of the zero frequency hydrodynamic Kramers form for *t*-stilbene in octanenitrile (dashed curve) and decanenitrile (solid curve). The reduced isomerization rates in octanenitrile (▲) and decanenitrile (●) are shown with error bars.

This article is copyrighted as indicated in the article. Reuse of AIP content is subject to the terms at: http://scitation.aip.org/termsconditions. Downloaded to IP: 130.88.90.140 On: Thu, 18 Dec 2014 22:34:06

TABLE III. Best fit Kramers parameters.

	E kcal/mol	$A(10^{12}\,s^{-1})$	B (cP)	ω_0[a] (cm^{-1})	ω_b[a] (cm^{-1})
t-stilbene					
n-octane	3.5	6.24	1.24	208	192
n-octanenitrile	2.6	1.35	3.62	45	561
4,4'-DMS					
n-octane	5.7	8.63	3.23	288	615
n-octanenitrile	4.2	2.31	1.92	77	366

[a] The major contribution to the error of these parameters is caused by systematic errors introduced by uncertainty in the barrier energy. A change in the barrier energy of $\pm$ 0.25 kcal/mol creates a change in the potential parameters of $\pm$ 50%.

Extended Kramers models

As discussed earlier, various workers have suggested the use of a frequency dependent friction in the Kramers equation, as appropriate. Grote and Hynes[32] have used a generalized Langevin equation which incorporates the frequency dependence of the friction in an expression for the rate constant in a consistent manner. Two approaches have been used to model this friction. First is the use of empirical solvent properties and a hydrodynamic model to compute the frequency dependent friction.[41] This friction is then used in the Grote–Hynes relation to model the reaction rate. In particular, this approach has been used for studies in the *n*-alkanes and provides good fits to the experimental data but unrealistic parameters for the intramolecular potential.[2,3] A second type of approach, which is phenomenological, has been proposed by Lee *et al.*[43,44] This approach assumes that when the solvent response is rapid compared to the solute motion the friction is treated adequately as proportional to the shear viscosity, but when the solvent response is slow the solute motion is independent of the shear viscosity of the solvent. Lee *et al.*[43,44] are able to fit this form to a wide range of data. In this section, the rate constants are fit to a modified Kramers form,[10,32] namely

$$\omega_b^2 - \lambda^2 = \frac{\lambda \zeta^*}{I_r} \tag{5}$$

which is identical to Eq. (2) with $\lambda = 2\pi\omega_b F(\zeta)/\omega_0$ and ζ^* is the friction for the isomerization process which may be a function of λ.

Bagchi and Oxtoby[33] proposed the use of a hydrodynamic model for the frequency dependent friction experienced by the isomerizing moiety. The mechanical model of the isomerization treats the isomerizing moiety as a sphere of radius R which is attached to the axis of rotation. The center of the sphere is a distance D from this axis.[33,39] The frequency dependent friction experienced by this sphere is

$$\zeta^* = \zeta(\lambda) = D^2 \zeta_{\rm tr}(\lambda) + \zeta_r(\lambda). \tag{6}$$

In this treatment a slip hydrodynamic boundary condition is used, and since the isomerizing moiety is modeled as a sphere, the rotational friction $\zeta_r(\lambda)$ is zero.[33] The modeling of the translational friction coefficient is that originally developed by Bixon and Zwanzing[41] and found to adequately describe the velocity autocorrelation function of small spheres. The translational friction $\zeta_{\rm tr}(\lambda)$ is given by

$$\zeta_{\rm tr}(\lambda) = \left(\frac{4\pi}{3}\right) \eta_s(\lambda) R X^2 [2(X+1)P + (1+Y)Q], \tag{7}$$

where

$$X = [\lambda \rho_0/\eta_s(\lambda)]^{1/2} R,$$

$$Y = \lambda \left(c^2 + \frac{\lambda \eta_l(\lambda)}{\rho_0}\right)^{-1/2} R,$$

$$P = \frac{3}{\Delta}(3 + 3Y + Y^2),$$

$$Q = \frac{3}{\Delta}\left(3 + 3X + X^2 + \frac{X^2(1+X)}{2 + \beta/\eta_s(\lambda)}\right),$$

$$\Delta = 2X^2[3 + 3Y + Y^2] + Y^2[3 + 3X + X^2] + \frac{3X^2(1+X)(2+2Y+Y^2)}{2 + \beta/\eta_s(\lambda)},$$

ρ_0 is the density, c is the velocity of sound, β is the hydrodynamic slip parameter (zero for a slip boundary condition and infinity for a stick boundary condition), $\eta_s(\lambda)$ is the frequency dependent shear viscosity, and $\eta_l(\lambda)$ is the frequency dependent longitudinal viscosity. The frequency dependent viscosities are modeled by a simple Maxwell form

$$\eta(\lambda) = \frac{\eta_0}{1 + \lambda\tau}, \tag{8}$$

where τ is a relaxation time which is modeled as η_0/G_∞ (G_∞ is the infinite frequency elastic modulus of the solvent). Some of these parameters are difficult to evaluate or to obtain, especially for the *n*-alkyl nitriles. In order to fit the data, average values were used for some of the parameters, namely $\rho_0 = 0.70$ g/cm^3 in *n*-alkanes, $\rho_0 = 0.85$ g/cm^3 in *n*-alkyl nitriles, $c = 1.0\times10^5$ cm/s, $\eta_l(\lambda) = 6\eta_s(\lambda)$, and $G_\infty = 10^{10}$ dyn/cm^2 which corresponds to 1 ps relaxation time for 1 cP viscosity. The quality of the fits to Eq. (7) for the data and the parameters obtained from these fits were found to be relatively insensitive to all of these parameters except G_∞. Variation of the densities over the full range for the liquid, variation of c by a factor of 2.5 and variation of η_l by a factor of 2 change the best fit parameters by less than 10%. However, the fits are very sensitive to G_∞ because it determines the solvent relaxation time.

Figure 6 shows a fit of the *t*-stilbene in *n*-alkyl nitriles data to Eq. (5) with ζ^* modeled in this way. The best fit parameters with $G_\infty = 10^{10}$ dyn/cm^2, $R = 3.2$ Å, $D = 2.5$

This article is copyrighted as indicated in the article. Reuse of AIP content is subject to the terms at: http://scitation.aip.org/termsconditions. Downloaded to IP: 130.88.90.140 On: Thu, 18 Dec 2014 22:34:06

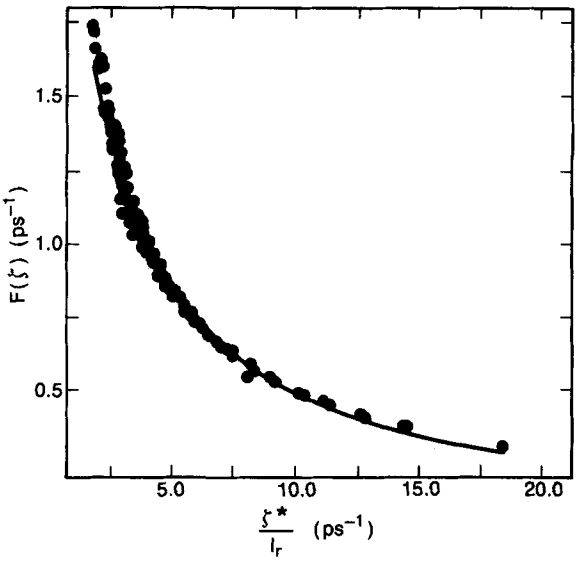

FIG. 6. Best fit of the reduced isomerization rate for *t*-stilbene in *n*-alkyl nitriles to a hydrodynamic frequency dependent friction model [Eq. (6)].

Å, and $I_r = 0.433 \times 10^{-44}$ kg m^2 are $\omega_b = 10$ cm^{-1} and $\omega_0 = 91$ cm^{-1}. If the value of G_∞ is lowered to 10^9 dyn/cm^2 the barrier frequency ω_b is lowered to 3.6 cm^{-1} and ω_0 increases to 125 cm^{-1}. If the value of G_∞ is increased to 3.0×10^{10} dyn/cm^2, the barrier frequency ω_b increases to 16 cm^{-1} and ω_0 decreases to 77 cm^{-1}. Further increases in the value of G_∞ leads to fits of notably less quality. The trend in the barrier parameters are qualitatively similar to those obtained by other workers[2(a),3(b)] for *t*-stilbene in *n*-alkanes and by Millar *et al.*[42] for 1,1'-binaphthyl in *n*-alkyl alcohols. That is, the barrier curvature is significantly more shallow than the well curvature. Use of a stick boundary condition in place of a slip boundary condition lowers the barrier frequency ω_b even further. It seems clear from the fits that since the reactive frequency λ is used to determine the friction the ratio ω_b/ω_0 is optimized for a good fit. When the value of G_∞ is decreased the ratio of frequencies is decreased in order to fit the data. Except for the case of $G_\infty = 3.0 \times 10^{10}$ dyn/cm^2, these frequencies are not realistic. However, these parameters do show a realistic trend between data sets (see Table IV). More specifically, as the barrier height increases for a given solute, the barrier curvature increases. This result is in direct contrast to the zero frequency result in which the trends were muddled.

Also shown in Table IV are the best fit parameters for both DMS and *t*-stilbene in a single solvent type. By assuming that the intramolecular potential has the same shape in both solutes it is possible to perform a three parameter fit to the combined data. Two of the parameters are the barrier frequencies for each solute and the third parameter is the ratio $2\pi\omega_b/\omega_0$, which should be the same for both solutes if the form of the potential does not change. Keeping this parameter fixed also has the benefit of keeping the characteristic relaxation time of the solvent fixed. An analysis of this sort probes the solvents' friction over a wider frequency range than a single solute analysis. Although the fits are quite good for both *n*-alkanes and *n*-alkyl nitriles the extracted potential parameters are once again unphysical, i.e., the barrier frequency is much too small for the corresponding well frequency. The ratio of the extracted parameters for the alkane results agree very well with the ratio of the barrier heights. However, the nitrile data yields barrier frequencies which are very similar despite a large difference in barrier height. Whether the failure of this model to extract reasonable parameters results from improper modeling of the frequency dependent friction on these time scales, the failure of hydrodynamics on this distance scale or the presence of multidimensional effects in the friction is unclear. Fits of the data in a single solvent to this friction model does not result in any improvement of the extracted parameters, nor does the use of a variable, i.e., subslip hydrodynamic boundary condition. These latter two variants are usually able to correct for the failures of hydrodynamics on a microscopic scale.

This interpretation of the parameters obtained from the fitting of the data to the frequency dependent friction case is strictly a one-dimensional interpretation of the reaction. That is, the influence of other modes are neglected. It is not unlikely that significant changes in the frequencies of other normal modes occur during isomerization. Incorporation of these changes results in the incorporation of an entropy term in the expression for the rate constant.[3,43–45] It now becomes ambiguous as to how ω_0 is determined. If ω_0 is assumed to be equal to ω_b in Table IV, then the frequencies would correspond to a physically reasonable potential energy surface (i.e., consistent with the barrier heights and moments of inertia). A method for estimating the entropy change has been described by Lee *et al.*[43] The changes in entropy required by these considerations are provided in Table IV as well and are found to be reasonable in magnitude. However, as pointed

TABLE IV. Potential parameters for fit to hydrodynamic frequency dependent friction model.[a]

System		E (kcal/mol)	ω_b (cm^{-1})	ω_0 (cm^{-1})	G_∞ (dyn/cm^2)	ΔS (cal/mol K)
DMS/lkanes		5.7	12	396	10^{10}	6.9
DMS/nitriles		4.2	9	130	10^{10}	5.3
t-stilbene/alkanes		3.5	11	299	10^{10}	6.6
t-stilbene/nitriles		2.6	10	91	10^{10}	2.2
Alkanes	*t*-stilbene	3.5	38	400	10^{10}	4.7
	DMS	5.7	49	517		
Nitriles	*t*-stilbene	2.6	34	174	10^{10}	3.2
	DMS	4.2	37	190		

[a] The structural parameters of *t*-stilbene and 4,4'-dimethoxystilbene (DMS) are the same as those used for the fits in Table III.

This article is copyrighted as indicated in the article. Reuse of AIP content is subject to the terms at: http://scitation.aip.org/termsconditions. Downloaded to IP: 130.88.90.140 On: Thu, 18 Dec 2014 22:34:06

out by Kim *et al.*,[3(b)] other studies indicate that ΔS should be very small for *t*-stilbene in *n*-alkanes.

A second model for the effective friction experienced by an isomerizing moiety has been proposed recently by Robinson and co-workers,[43,44] and it is found to fit both experimental data and molecular dynamics simulations quite well. In particular, these workers propose the use of

$$\zeta^* = \frac{A_0 \omega_b I_r}{F(\zeta)} \left(\frac{\eta_0}{a + b\eta_0} \right) \tag{9}$$

for the effective friction, where A_0, a, and b are adjustable parameters. At very low viscosities this equation follows Stokes law and the friction is proportional to η_0 whereas at high viscosities the friction saturates and becomes independent of shear viscosity. The ratio of frequency factors incorporates a frequency dependence in an approximate way as well. As $F(\zeta)$ becomes large at low viscosities ζ^* will decrease and at high viscosities when $F(\zeta)$ is small the friction will increase as $1/F(\zeta)$. The extra parameter A_0 is a factor "to account for any entropy contributions caused by deviations from the one-dimensional picture." [43] In order to compare this analysis with the earlier work of Lee *et al.*,[43] it is useful to write Eq. (5), with the friction given by Eq. (9), as

$$F(\zeta) = A_1 \left[\frac{P/\eta_0 + R - 1}{P/\eta_0 + R + 1} \right]^{1/2}, \tag{10}$$

where $A_1 = A_0\omega_0/2\pi$, $P = 2aA_1$, and $R = 2bA_1 - 1$. Table V shows the best fit parameters for fits of this model to the data. The best fit curves of this model to the data are given in Fig. 3 for *t*-stilbene and Fig. 4 for 4,4′-dimethoxystilbene. The parameters P and R do not follow the trends which Lee *et al.* observed for other systems. Although the parameter P increases with increase in the size of the isomerizing moiety, the value of R does not approach its limiting value of unity. The value of R is larger for 4,4′-dimethoxystilbene than for *t*-stilbene. The trend in the P parameter only holds within a solvent type, however. Since P is a measure of the solute/solvent coupling, the increase in P for the alkanes over the nitriles could be a result of a changing hydrodynamic boundary condition.

As Lee *et al.* show, it is possilbe to reexpress Eq. (10) in a Kramers form with an effective viscosity η^*. The effective viscosity has the form

$$\eta^* = g\eta_0[1 + 2R\eta_0/P + (R^2 - 1)\eta_0^2/P^2]^{-1/2},$$

where

$$g = \frac{2\omega_b I_r}{fDR^2 P}$$

and f is 4π for a slip boundary condition and 6π for a stick boundary condition. As η_0 becomes small η^* is proportional to η_0 with a proportionality constant g. By modeling the form of the potential in the manner described by Lee, namely $\omega_0 = \omega_b = \sqrt{2E/I_r}$, and using the previously given values of the other parameters a value of g can be obtained. The parameter g is the limiting value of the viscosity dependence. As seen from the values in Table V it seems to be highly correlated with the barrier height. As the barrier height in a given solvent type increases the value of g drops, primarily because the value of P increases. This trend indicates that even though a larger group is moving through the solvent it experiences less friction than a smaller group moving at a slower speed, i.e., frequency dependent effects of the friction win out over spatial effects. Between solvent types, however, this trend does not hold, DMS in nitriles has a larger value of g than *t*-stilbene in alkanes despite the fact that DMS has a higher barrier. This behavior may result from stronger solute/solvent coupling, which could be a result of the increased solute/solvent size ratio and/or stronger attractive interactions between the solute and the nitriles as compared to the solute and the alkanes. In hydrodynamic terms this would correspond to a change in the boundary condition.

Coupled oscillator model

In a series of papers van der Zwan and Hynes have treated the relative motion of two coupled dipoles in a dipolar solvent.[45,46] Their treatment is based on a generalized Langevin description of the motion and friction as outlined by Grote and Hynes.[10,32] This treatment assumes a particular form for the time dependent friction and models the solute/solvent interaction via an oscillator model. Although a simple model and developed in terms of dipolar coupling, it should model general features of the reaction dynamics and should be applicable to nonpolar solvents. Van der Zwan and Hynes consider a variety of cases, but the most appropriate for this study is the overdamped solvent regime, which results in an expression of the form

$$\lambda^2 - \omega_{b,eq}^2 + \frac{\omega_{b,eq}^2 \beta \lambda \tau_s}{1 + \lambda\tau_s} = 0. \tag{11}$$

The quantity λ is the reactive frequency which is given by $\omega_{b,eq}\kappa$, where κ is the transmission coefficient (ratio of actual rate constant to the transition state theory predictions) and $\omega_{b,eq}$ is the frequency of the equilibrium solvated barrier. This frequency would determine the reactive frequency in

TABLE V. Parameters obtained from fits to Eq. (10).

System	A_1[a] (10^{12} s^{-1})	P[a] (10^{-2} cP)	R[b]	E (kcal/mol)	g
DMS/alkanes	11.4	58.1	1.221	5.7	0.161
DMS/nitriles	5.6	12.9	1.005	4.2	0.624
t-stilbene/alkanes	10.1	19.3	1.060	3.5	0.476
t-stilbene/nitriles	6.5	6.2	0.998	2.6	1.28

[a] The best fit values of these parameters can change by a factor of 2 for changes in the barrier height of $\pm$ 0.25 kcal/mol.

[b] The best fit values of these parameters can change by $\pm$ 0.01 for changes in the barrier height of $\pm$ 0.25 kcal/mol.

This article is copyrighted as indicated in the article. Reuse of AIP content is subject to the terms at: http://scitation.aip.org/termsconditions. Downloaded to IP: 130.88.90.140 On: Thu, 18 Dec 2014 22:34:06

the limit that the solute and solvent remained in equilibrium. The quantity τ_s is a characteristic solvent relaxation time which determines the friction on the barrier crossing, and β is a measure of the solute/solvent coupling strength. The quantity λ is the reactive frequency, which in terms of $F(\zeta)$ is given as

$$\lambda = \frac{2\pi F(\zeta)\omega_{b,\mathrm{eq}}}{\omega_0}\left(\frac{\omega_s}{\omega_{\mathrm{so}}}\right), \tag{12}$$

where ω_0 is the frequency of the reactant well, ω_{so} is the characteristic solvent frequency when the solute is in the reactant well, and ω_s is the characteristic frequency of the solvent when the solute is at the transition state. In the nonpolar alkane solvents these latter two frequencies should be similar, whereas for the dipolar nitrile solvents they could significantly differ. It is useful to note that Eq. (11) has the same form as Eq. (5) with

$$\frac{\zeta^*}{I_r} = \frac{\omega_{b,\mathrm{eq}}^2 \beta \tau_s}{1+\lambda\tau_s}$$

and the barrier frequency ω_b replaced by the equilibrium solvated barrier frequency $\omega_{b,\mathrm{eq}}$. This form of ζ^* is a Maxwell form, as was the case in the modeling of the hydrodynamic friction. This model differs from the hydrodynamic model by its use of a microscopic relaxation time and a solute/solvent coupling which is an adjustable parameter (this model has three parameters).

Because of the number of parameters in Eq. (11) it is difficult to fit the data to the fully parametrized equation without obtaining pathological values for the parameters. Consequently, in comparing the data with Eq. (11), it is assumed that $F(\zeta)$ is the reactive frequency λ. For the *n*-alkyl nitriles τ_s is modeled by τ_d the Debye dielectric relaxation time. The procedure followed for estimating τ_d is the same as that described previously. For the *n*-alkanes it is possible to estimate τ_s via G_∞ as outlined earlier, but it is also possible to use light scattering relaxation times τ_{ls} for the solvent.[7] Although both procedures give reasonable fits, the use of τ_{ls} is given here.

The parameters obtained from the fits of the data to Eq. (11) have realistic values and show the correct sort of trend (see Table VI). Figure 7 shows the relative error for a fit of the *t*-stilbene data in *n*-alkyl nitriles with τ_d as a measure of the solvent relaxation time. It is clear from Fig. 7 that although the fitted values agree with the experimental values to within experimental error, the deviations are not random.

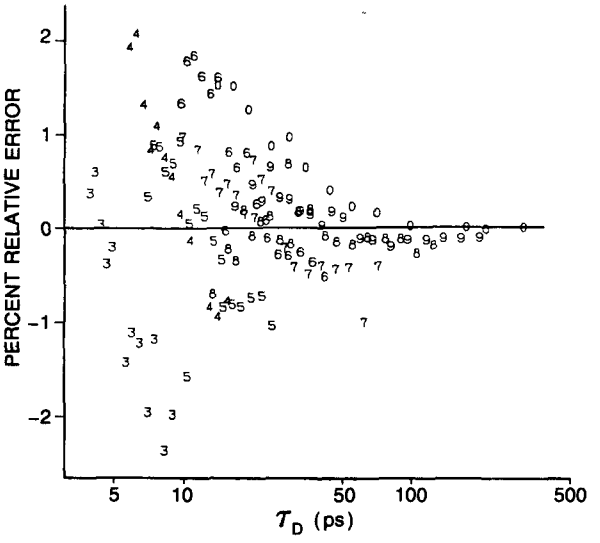

FIG. 7. Best fit of the *t*-stilbene in *n*-alkyl nitriles data to the coupled oscillator model [Eq. (11)]. Each number in the plot corresponds to a data point where the solvent has the corresponding number of carbon atoms (except for decanenitrile which is represented by a 0).

Each type of solvent (represented by a number corresponding to the number of carbon atoms in the solvent molecule) shows systematic deviations from the data. Figure 8 shows a simultaneous fit for *t*-stilbene and 4,4'-dimethoxystilbene in *n*-alkyl nitriles with τ_d used as the solvent relaxation time. The use of τ_l (longitudinal dielectric relaxation time, $\tau_l = \tau_d \epsilon_\infty / \epsilon_0$) as a measure of the solvent relaxation provides worse fits. The value of β seems to change, but not very dramatically, with solvent type (alkanes vs nitriles). Also, the values of $\omega_{b,\mathrm{eq}}$ seem to correlate properly with barrier height in a given solvent type and have magnitudes which are reasonable for torsional frequencies. The fact that the frequencies do not correlate between solvent types could indicate that the energy barriers to the isomerization obtained from the isoviscosity plots are not "equilibrium" barriers but incorporate nonequilibrium effects in an average way. This latter conclusion requires better quantitative examination of this model before it can be considered more than conjecture.

Also, Table VI contains the parameter $\zeta(t=0)$ which corresponds to the magnitude of the solute/solvent frictional coupling at time zero and is given by $\omega_{b,\mathrm{eq}}^2\beta$.[45] This

TABLE VI. Best fit of the data to Eq. (11) with $F(\zeta) = \lambda$.

System		$\omega_{b,\mathrm{eq}}$ (cm^{-1})	β	$\zeta(t=0)$ (ps^{-2})
Stilbene/alkanes ($\tau_s = \tau_{\mathrm{ls}}$)		91	0.965	284
Stilbene/nitriles ($\tau_s = \tau_d$)		27	1.01	26
DMS/alkanes ($\tau_s = \tau_{\mathrm{ls}}$)		185	0.968	1177
DMS/nitriles ($\tau_s = \tau_d$)		38	0.996	51
Alkanes ($\tau_s = \tau_{\mathrm{ls}}$)	*t*-stilbene	123	0.988	531
	DMS	157	0.950	832
Nitriles ($\tau_s = \tau_d$)	*t*-stilbene	29	1.011	30
	DMS	37	0.994	48

This article is copyrighted as indicated in the article. Reuse of AIP content is subject to the terms at: http://scitation.aip.org/termsconditions. Downloaded to IP: 130.88.90.140 On: Thu, 18 Dec 2014 22:34:06

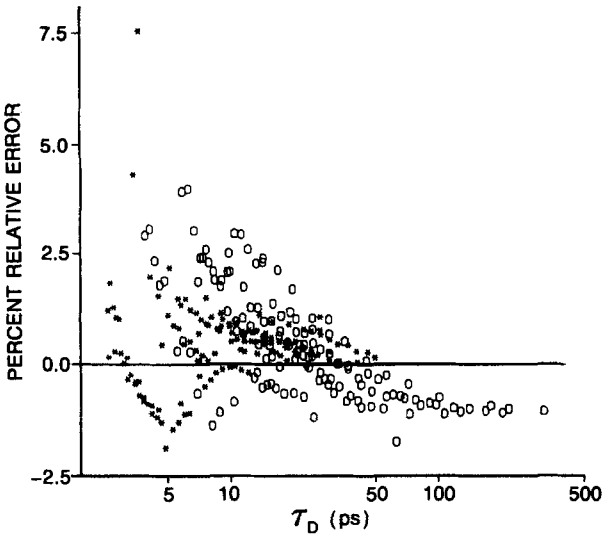

FIG. 8. Best fit of the coupled oscillator model [Eq. (11)] to reduced isomerization rate data for *t*-stilbene in *n*-alkyl nitriles (○) and dimethoxystilbene in *n*-alkyl nitriles (*).

latter quantity is found to be much larger for the alkanes than for the nitriles; a result which seems unrealistic. This result could come from a variety of sources: unrealistic β parameters, the inadequacy of modeling λ as $F(\zeta)$ instead of the more proper expression, and/or differences in τ_{ls} and τ_d as measures of the solvent relaxation time. If τ_s is assumed to be proportional to η_0 (instead of τ_{ls} or τ_d) and the proportionality constant is varied in a fit to Eq. (11), the friction at zero time $\zeta(t=0)$ shows the correct trend between solvent types (i.e., larger for the *n*-alkyl nitriles than for the *n*-alkanes). The assumption that $F(\zeta)$ is the reactive frequency implies that $\omega_o = 2\pi\omega_{b,eq}$, if $\omega_{so} = \omega_s$ in Eq. (12). Using the values of $\omega_{b,eq}$ given in Table VI, reactant well frequencies are obtained which are quite unrealistic for a torsional potential. If the fit of the data to the model is restricted to more realistic potential parameters, poor agreement is found. In conclusion, the same trends are observed here as are seen in comparison with the hydrodynamic friction model. Namely, the reactant well frequency is too large for the corresponding barrier frequency.

In summary, the inadequacies of a stochastic one-dimensional model which are seen in other systems are observed for *t*-stilbene in nitriles and 4,4′-dimethoxystilbene in nitriles. Non-Markovian effects can be incorporated into the treatment of the dynamics via a frequency dependent friction. The use of hydrodynamic frequency dependent friction fits the data quite well but with unrealistic potential parameters and is very sensitive to the relaxation time used for the solvent friction. Similar effects have been observed by other workers. Most notably, Millar *et al.*[42] find that even though a zero frequency hydrodynamic model of the friction shows good agreement with Kramers model, a frequency dependent hydrodynamic friction model fails to give good fits to the data unless unrealistic potential parameters are used. This observation is suggestive of a breakdown in the hydrodynamic approximation on the time scale of reaction. The use of a more microscopic modeling of the frequency dependent friction in the coupled oscillator model provides a better fit to the data, but with unreasonable potential parameters, as well. A caveat of this analysis is that the microscopic dielectric relaxation time was estimated in higher alkyl nitrile solvents via fits to acetonitrile data and the use of the hydrodynamic approximation. It is important to realize that a frequency dependent friction model yields reasonable potential parameters if entropic effects are invoked. This explanation is equivalent to a breakdown of the one-dimensional approximation and quite reasonable because of the presence of many other nonreactive modes in the solute molecule. Lastly, a modeling not explored in the analysis here is the

APPENDIX. Measured viscosities of *n*-alkyl nitriles.

IA:

	η(cP)	T(°C)	η(cP)	T(°C)	η(cP)	T(°C)
Propionitrile	0.729	−20.0	0.638	−10.0	0.556	0.0
Butanenitrile	1.069	−19.0	0.905	−10.0	0.776	0.0
Pentanenitrile	1.453	−20.0	1.199	−10.0	1.009	0.0
Hexanenitrile	2.142	−20.0	1.703	−10.0	1.383	0.0

IB:

Heptanenitrile		Octanenitrile		Nonanenitrile		Decanenitrile	
T(°C)	η(cP)	T(°C)	η(cP)	T(°C)	η(cP)	T(°C)	η(cP)
−20.0	3.106	−19.0	4.642	−19.0	6.489	−20.0	9.665
−10.0	2.346	−9.5	3.356	−9.5	4.565	−11.0	6.523
0.0	1.845	0.0	2.540	0.0	3.363	0.0	4.577
2.0	1.795	10.0	2.030	9.5	2.694	10.0	3.464
10.0	1.507	20.0	1.651	18.5	2.152	20.0	2.676
20.0	1.259	29.5	1.368	23.5	1.844	29.5	2.140
29.5	1.064	39.0	1.158	28.5	1.707	39.0	1.747
39.5	0.917	45.5	1.048	39.0	1.403	50.0	1.432
50.0	0.788	59.5	0.863	49.5	1.187	60.0	1.220
60.5	0.692	70.5	0.743	59.0	1.023	70.0	1.055
70.0	0.617	82.0	0.650	70.0	0.886	80.0	0.927
80.0	0.555			79.5	0.784		

Estimated error in η is $\pm$ 0.01 cP, and in T is $\pm$ 0.05 °C.

This article is copyrighted as indicated in the article. Reuse of AIP content is subject to the terms at: http://scitation.aip.org/termsconditions. Downloaded to IP: 130.88.90.140 On: Thu, 18 Dec 2014 22:34:06

presence of more than one reactive mode,[47] which has been shown theoretically to explain the trend observed in the power law of the reduced isomerization rates' viscosity dependence.

CONCLUSIONS

This work provides new results for isomerization dynamics in polar solvents. In contrast to recent studies in alcohol solvents (associated), the homologous series of *n*-alkyl nitriles (unassociated) allows an activation barrier to be identified for the isomerization. This result implies that viscosity is not the determining factor in the modification of barrier heights in the stilbenes. This barrier is solvated by dielectric interactions with the solvent, in agreement with expectations. Although the description of isomerization dynamics in alcohol solvents may necessarily involve a multidimensional model, in the nitriles it is possible to discuss an effective one-dimensional potential energy surface.

The same type of deviations of the data from the predictions of a stochastic Kramers model are observed here as are observed in nonpolar solvents. More detailed treatment of the solute/solvent frictional coupling provides better agreement with the experimental data, however, the parameters obtained from this modeling are not always in agreement with physical expectations. The best fit of the data comes from comparison with a coupled oscillator model of the isomerization.

ACKNOWLEDGMENTS

We thank J. Brady for the use of the SLM 8000 fluorimeter and Beckman DU7 absorption spectrometer as well as numerous discussions. We thank G. R. Fleming and S. Kim for providing us with the raw data for *t*-stilbene in *n*-alkanes. This research was supported by the donors of the Petroleum Research Fund, administered by the American Chemical Society and by NSF Grant No. CHE-8613468.

[1]R. M. Hochstrasser, Pure Appl. Chem. **52**, 2683 (1980).
[2](a) G. Rothenberger, D. K. Negus, R. M. Hochstrasser, J. Chem. Phys. **79**, 5360 (1983); (b) M. Lee, A. J. Bain, P. J. McCarthy, C. H. Han, J. N. Haseltine, A. B. Smith III, and R. M. Hochstrasser, *ibid.* **85**, 4341 (1986).
[3](a) S. H. Courtney and G. R. Fleming, J. Chem. Phys. **83**, 215 (1985); (b) S. K. Kim and G. R. Fleming, J. Phys. Chem. **92**, 2168 (1988).
[4](a) G. R. Fleming, S. H. Courtney, and M. W. Balk, J. Stat. Phys. **42**, 83 (1986); (b) M. Lee, G. R. Holtom, and R. M. Hochstrasser, Chem. Phys. Lett. **118**, 359 (1985).
[5]J. M. Hicks, M. T. Vandersall, E. V. Stizmann, and K. B. Eisenthal, Chem. Phys. Lett. **135**, 413 (1987).
[6]V. Sundström and T. Gillbro, Chem. Phys. Lett. **109**, 538 (1984).
[7]D. M. Zeglinski and D. H. Waldeck, J. Phys. Chem. **92**, 692 (1988).
[8](a) K. J. Smit and K. P. Ghiggino, Chem. Phys. Lett. **122**, 369 (1985); (b) J. B. Hopkins and P. M. Rentzepis, *ibid.* **124**, 79 (1986).
[9]H. A. Kramers, Physica **7**, 284 (1940).
[10](a) J. T. Hynes, *Theory of Chemical Reactions* (Chemical Rubber, New York, 1985), p. 171; (b) J. Stat. Phys. **42**, 149 (1986).
[11]B. J. Berne, M. Borkovec, and J. E. Straub, J. Phys. Chem. **92**, 3711 (1988).
[12](a) T. J. Majors, U. Even, and J. Jortner, J. Chem. Phys. **81**, 2330 (1984); (b) J. Syage, W. Lambert, P. Felker, A. H. Zewail, and R. M. Hochstrasser, Chem. Phys. Lett. **88**, 266 (1982).
[13]L. Salem, *Electrons in Chemical Reactions* (Wiley, New York, 1982), p. 74.
[14]K. M. Keery and G. R. Fleming, Chem. Phys. Lett. **89**, 322 (1982).
[15]J. Hicks, M. Vandersall, Z. Babarogic, and K. B. Eisenthal, Chem. Phys. Lett. **116**, 18 (1985).
[16]E. Akesson, V. Sundström, T. Gillbro, Chem. Phys. Lett. **121**, 513 (1985); Chem. Phys. **106**, 269 (1986).
[17]P. F. Barbara, Acc. Chem. Res. **21**, 195 (1988).
[18]M. A. Kahlow, T. J. Kang, and P. F. Barbara, J. Chem. Phys. **83**, 5076 (1985).
[19]D. V. O'Connor and D. Phillips, *Time Correlated Single Photon Counting* (Academic, New York, 1984).
[20](a) S. R. Meech and D. Phillips, J. Photochem. **23**, 193 (1983); (b) J. N. Demas and G. A. Crosby, J. Phys. Chem. **75**, 991 (1971); (c) W. H. Melhuish, *ibid.* **65**, 229 (1961).
[21](a) J. A. Riddick, W. B. Bunger, and T. K. Sakano, *Techniques of Chemistry, Organic Solvents*, 4th ed. (Wiley, New York, 1986); (b) D. D. Perrin, W. L. F. Armarego, and D. R. Perrin, *Purification of Laboratory Chemicals*, 2nd ed. (Pergamon, New York, 1982).
[22](a) L. Deffet, Bull. Soc. Chem. Belg. **7**, 391 (1931); (b) L. H. Thomas, Chem. Eng. J. **11**, 20 (1976); (c) J. Timmermans, *Physico-Chemical Constants of Pure Organic Compounds* (Elsevier, New York, 1965) Vols. 1 & 2; (d) Landolt-Bornstein, *Zahlenwerte and Funktionen* (Springer, New York, 1967).
[23](a) R. R. Dreisbach, in *Physical Properties of Chemical Compounds* (American Chemical Society, Washington, D.C., 1961), Adv. Chem. Ser. No. 29. (b) *International Critical Tables* (Maple, York, PA, 1930).
[24]A. J. Cross and G. R. Fleming, Biophys. J. **46**, 45 (1984).
[25]C. Reichardt, *Solvent Effects in Organic Chemistry, Monographs in Modern Chemistry*, Vol. 3, edited by H. F. Ebel (Springer, New York, 1979).
[26]J. E. Brady and P. W. Carr, J. Phys. Chem. **89**, 1813 (1985).
[27](a) G. P. Srivastava, P. C. Mathur, and K. N. Tripathi, Ind. J. Pure Appl. Phys. **9**, 364 (1971); (b) J. K. Eloranta and P. K. Kadaba, Chem. Phys. Lett. **11**, 251 (1971); (c) Trans. Faraday Soc. **66**, 817 (1970); (d) J. M. Dereppe and M. van Meersche, Bull. Soc. Chim. Belg. **69**, 466 (1960).
[28]R. M. Bowman, K. B. Eisenthal, and D. P. Millar, J. Chem Phys. **89**, 762 (1988).
[29]S. P. Velsko, D. H. Waldeck, and G. R. Fleming, J. Chem. Phys. **78**, 249 (1983).
[30](a) S. P. Flom, V. Nagarajon, and P. F. Barbara; J. Phys. Chem. **90**, 2085 (1986); (b) P. F. Barbara and G. C. Walker, Rev. Chem. Intermed. **10**, 1 (1988).
[31]G. R. Fleming, D. H. Waldeck, K. M. Keery, and S. P. Velsko, *Applications of Picosecond Spectroscopy to Chemistry*, edited by K. B. Eisenthal (Reidel, Dordecht, 1984).
[32]R. F. Grote and J. T. Hynes, J. Chem. Phys. **74**, 4465 (1981).
[33](a) B. Bagchi, Int. Rev. Phys. Chem. **6**, 1 (1987); (b) B. Bagchi and D. W. Oxtoby, J. Chem. Phys. **78**, 2735 (1983).
[34]D. Gegiou, K. A. Muszkat, and E. Fischer, J. Am. Chem. Soc. **90**, 12 (1968).
[35](a) D. Ben-Amotz and J. M. Drake, J. Chem. Phys. **89**, 1019 (1988); (b) D. Ben-Amotz and T. W. Scott, J. Chem. Phys. **87**, 3739 (1987).
[36](a) J. L. Dote, D. Kivelson, and R. N. Schwartz, J. Phys. Chem. **85**, 2169 (1981); (b) L. A. Phillips, S. P. Webb, and J. H. Clark, J. Chem. Phys. **83**, 5810 (1985); (c) D. H. Waldeck and G. R. Fleming, J. Phys. Chem. **85**, 2614 (1981).
[37](a) P. Debye, *Polar Molecules* (Dover, New York, 1956); (b) H. Frohlich, *Theory of Dielectrics* (Oxford, Oxford, 1986).
[38](a) A. B. Myers, M. A. Pereira, P. L. Holt, and R. M. Hochstrasser, J. Chem. Phys. **86**, 5146 (1987); (b) K. Tanabe and J. Hiraishi, Mol. Phys. **39**, 493 (1980).
[39]J. S. McCaskill and R. G. Gilbert, Chem. Phys. **44**, 389 (1979).
[40]C. -M. Hu and R. Zwanzig, J. Chem. Phys. **60**, 4354 (1974).
[41](a) R. Zwanzig and M. Bixon, Phys. Rev. A. **2**, 2005 (1970); (b) H. Metiu, D. W. Oxtoby, and K. F. Freed, Phys. Rev. A. **15**, 361 (1977).
[42]D. P. Millar and K. B. Eisenthal, J. Chem. Phys. **23**, 5076 (1985).
[43]J. Lee, S. B. Zhu, and G. W. Robinson, J. Phys. Chem. **91**, 4273 (1987).
[44](a) S. B. Zhu, J. Lee, G. W. Robinson, and S. H. Lin, Chem. Phys. Lett. **148**, 164 (1988); (b) S. B. Zhu, J. Lee, and G. W. Robinson, J. Chem. Phys. **88**, 7088 (1988).
[45]G. van der Zwan and J. T. Hynes, Chem. Phys. **90**, 21 (1984).
[46](a) G. van der Zwan and J. T. Hynes, J. Chem. Phys. **78**, 4174 (1983); (b) **76**, 2993 (1982); (c) Chem. Phys. Lett. **101**, 367 (1983).
[47]N. Agmon and R. Kosloff, J. Phys. Chem. **91**, 1988 (1987).

This article is copyrighted as indicated in the article. Reuse of AIP content is subject to the terms at: http://scitation.aip.org/termsconditions. Downloaded to IP: 130.88.90.140 On: Thu, 18 Dec 2014 22:34:06